# Bayesian model comparison and distinguishability

**Julien Diard (julien.diard@upmf-grenoble.fr)**
Laboratoire de Psychologie et NeuroCognition CNRS-UPMF
Grenoble, France

## Abstract

This paper focuses on Bayesian modeling applied to the experimental methodology. More precisely, we consider Bayesian model comparison and selection, and the *distinguishability* of models, that is, the ability to discriminate between alternative theoretical explanations of experimental data. We argue that this last concept should be central, but is difficult to manipulate with existing model comparison approaches. Therefore, we propose a preliminary extension of the Bayesian model selection method that incorporates model distinguishability, and illustrate it on an example of modeling the planning of arm movements in humans.

**Keywords:** Bayesian modeling; model selection; distinguishability; arm movement; trajectory planning; human control.

## Notation

| | |
|---|---|
| $\delta$ | a single data point |
| $\Delta$ | a set of data points |
| $x, y$ | coordinates for data points |
| $m_i$ | a single model (the $i$-th) |
| $M$ | a set of models |
| $\theta$ | a single parameter value |
| $\Theta$ | a set of parameter values |
| $D$ | measure of distinguishability |

## Introduction

In probabilistic modeling, models are usually encoded by a term that describes the probability of an experimental datum $\delta$, given the model $M_i$: $P(\delta \mid M_i)$.

When the purpose is to select a model out of several alternatives, given some observed data points, the $P(\delta \mid M_i)$ term is usually hierarchically encapsulated in a higer-level model, which relates several models $M$, several possible parameter values for these models $\Theta$, and several data points $\Delta$:

$$P(M \, \Delta \, \Theta) = P(M)P(\Theta \mid M)P(\Delta \mid \Theta \, M) \ . \tag{1}$$

This leads to a variety of interesting model selection techniques, like the Maximum Likelihood Estimator (MLE), the Maximum A Posteriori estimator (MAP), various least squares based estimators, or algorithms using the Akaike Information Criterion (AIC), the Bayesian Information Criterion (BIC), or, more generally, the Bayesian Model Selection method (BMS). We refer the interested reader to previous reviews of these techniques (Myung & Pitt, 2004; Hélie, 2005).

All of these methods, at their core, aim at selecting a model out of a class of models, in order to maximize the fit measure, or some compound of the fit and model complexity. One of the possible extensions is, instead of selecting one single model, to consider the whole distributions over models $P(M \mid \Delta)$ in order to gain a better understanding of the relation between the best model and the next best models. The issues here are legitimate: how is the best model winning over the rest? Is it only marginally better?

However, some further questions, that are relevant in terms of scientific methodology, cannot easily be treated on the basis of Eq. (1) alone. Indeed, it is a very simple structure, which places at the heart of the analysis the fit of a single datum $\delta_i$ to a single model $m_j$, in the term $P(\delta_i \mid [M = m_j])$.

For instance, a couple of questions, that are crucial for the scientific methodology, are: "are $m_i$ and $m_j$ predicting different results?", and "where should the next experiment investigate in order to clarify whether $m_i$ or $m_j$ is the best model?". In other words, the central issue here is the *distinguishability* of models $m_i$ and $m_j$ (Berthier, Diard, Pronzato, & Walter, 1996) [1], in particular with respect to the space of experimental data. Instead of caring about the particular fit, or lack thereof of a model, the concern is about the relative fits of available models; are models with relatively close fits able to being discriminated, or not? The two above questions could then be translated mathematically by $P(\text{distinguishable} \mid [M_1 = m_1] \, [M_2 = m_2])$ and $P(x_{T+1} \mid [\text{distinguishable} = 1])$ (using an informal notation for the moment).

However, it appears that Eq. (1) is too limited to allow for an easy formulation of the inclusion of the distinguishability of models. The fit and experimental adequacy of a model, in science, is a complex concept; capturing this rich and difficult concept in a single number that would form the basis of an absolute ranking might be a red herring. Indeed, even the composition of the notion of fit and generalization into a single measure has proven a challenging task for a wide variety of modeling approaches, even though the two concepts are related. Therefore, we propose to pursue an alternate route, developing explicit mathematical formulations of the measure of interest, so as to allow their principled manipulation, using Bayesian inference.

Therefore, we propose to extend here the hierarchical model of Eq. (1) so as to incorporate the notion of distinguishability of models. The central component is to augment the model fit term with a model comparison term.

In the remainder of this paper, we develop the theoretical distinguishability analysis Bayesian model, illustrate it on a hypothetical example, and finally apply it to a scientifically relevant area, the modeling of the planning of arm movements in humans.

## Bayesian model distinguishability

Let $m_1$ and $m_2$ be two models under consideration. Consider a data space where $x$ are inputs, and models $m_1$ and $m_2$ predict outputs $y_1$ and $y_2$, respectively, according to the term

---

[1] This is not a self reference, despite the homonymy of the second author.
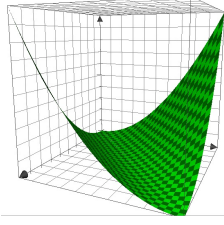
Figure 1: $P(D = 1 \mid x\,y\,M_1\,M_2\,\Theta_1\,\Theta_2)$ plotted against $P(M = M_1\,\Theta = \theta_1 \mid x\,y)$ and $P(M = M_2\,\Theta = \theta_2 \mid x\,y)$.

$P(y \mid x\,\theta\,M)$, which is the general likelihood term. Let $D$ be a probabilistic variable, that is binary: it can take values 1 if the models are distinct, and 0 if the models are not distinct. Therefore, we are interested in $P(D \mid x\,y\,\theta_1\,M_1\,\theta_2\,M_2)$: what is the probability that the models are distinguishable given an experimental point $x, y$ and two models?

We define the hierarchical model of model comparison, our alternative to Eq. (1) for the purpose of manipulating distinguishability, as follows:

$$
\begin{aligned}
&P(D\,x\,y\,M_1\,M_2\,\Theta_1\,\Theta_2) \\
&= \quad P(M_1\,M_2)P(\Theta_1 \mid M_1)P(\Theta_2 \mid M_2) \\
&\qquad P(x)P(y \mid x\,M_1\,M_2\,\Theta_1\,\Theta_2) \\
&\qquad P(D \mid x\,y\,M_1\,M_2\,\Theta_1\,\Theta_2)
\end{aligned}
$$

We call the term $P(D \mid x\,y\,M_1\,M_2\,\Theta_1\,\Theta_2)$ the *a posteriori distinguishability*, because it is the distinguishability of $M_1$ and $M_2$ with respect to some already observed data point $x, y$, as opposed to $P(D \mid M_1\,M_2\,\Theta_1\,\Theta_2)$, which is the *a priori distinguishability* of $M_1$ and $M_2$, irrespective of any data point. The latter will be obtained via Bayesian inference from the former, as shown below.

### *a posteriori* distinguishability

**Model** We define $P(D \mid x\,y\,M_1\,M_2\,\Theta_1\,\Theta_2)$ as follows:

$$
\begin{aligned}
&P(D = 1 \mid x\,y\,M_1\,M_2\,\Theta_1\,\Theta_2) = \\
&\sqrt{(P(M = M_1\,\Theta = \theta_1 \mid x\,y) - P(M = M_2\,\Theta = \theta_2 \mid x\,y))^2}\,.
\end{aligned}
$$

It is illustrated Fig. 1 [2]

This measure of distance between model recognition given an experimental data has some interesting properties; for instance, the probability that $D = 1$ is 0 if and only if the probabilities $P(M = M_1\,\Theta = \theta_1 \mid x\,y)$ and $P(M = M_2\,\Theta = \theta_2 \mid x\,y)$ are equal. The probability that $D = 1$ is 1 if and only if either one of $P(M = M_1\,\Theta = \theta_1 \mid x\,y)$ and $P(M = M_2\,\Theta = \theta_2 \mid x\,y)$ is 1 and the other is 0.

---

[2]Alternative definitions, based on other $L_p$ norms, do exist and have been explored experimentally. For instance, we also used the absolute distance of the difference (the $L_1$ norm). However, these alternate definitions do not appear to yield dramatically different results. The issue of the *distinguishability of distinguishability measures* is a topic for further research.
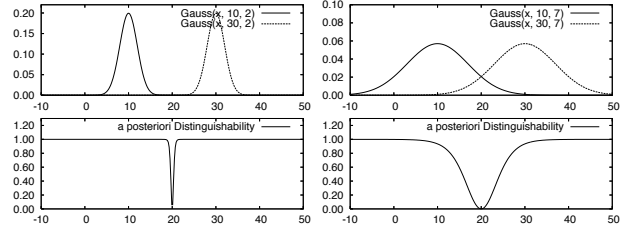


Figure 2: Left: The models are clearly distinguishable. Right: In case of higher standard deviation, the indistinguishability gap between the predictions is wider.
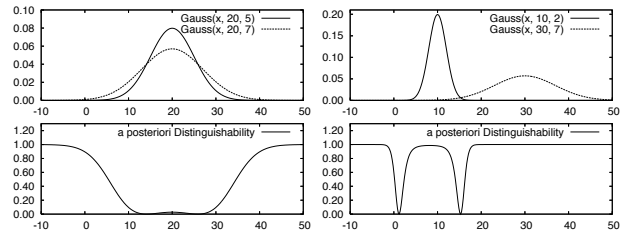


Figure 3: Left: Hardly distinct models (gaussian distributions with same means and close standard deviations). Right: Models with different means and different standard deviations. Note the asymmetry of the bump of distinguishability around the left gaussian model, which corresponds to the cases where it is recognized as the correct model.

Another property of our measure of distinguishability is to be noted: it is symmetric with respect to $M_1$ and $M_2$, contrary to previous approaches (Navarro, Pitt, & Myung, 2004).

Finally, since $D$ is a binary variable, we easily turn our distinguishability into a probability measure by defining $P(D = 0 \mid .) = 1 - P(D = 1 \mid .)$: *a posteriori* distinguishability integrates to one. Therefore, the probability distributions over $D$ can fully be described by a single number. By convention, in the remainder of the paper, we only focus on $P(D = 1 \mid .)$.

**Example** We give a straightforward example, in order to illustrate the a posteriori distinguishability of models.

We define two models $m_1$ and $m_2$, of the same family of models, both being defined by Gaussian probability distributions over some arbitrary unit. We set $x$ to some arbitrary value for the moment, in order to have a mono-dimensional data point, over $y$. Finally, we only consider two possible sets of parameters $\theta_1$ and $\theta_2$. In the following figures, we show how $P(D \mid x\,y\,M_1\,M_2\,\Theta_1\,\Theta_2)$ evolves as a function of $y$, in different cases for $\theta_1$ and $\theta_2$.

The first example is when the two models clearly predict different outcomes over $y$. The Gaussian probability distributions for $m_1$ and $m_2$ are centered on values $\mu_1$ and $\mu_2$ that are far apart, in the sense that $\mu_1 - \mu_2 \gg \sigma_1$ and $\mu_1 - \mu_2 \gg \sigma_2$. This case is shown Fig. 2 (left). It can be seen that the distinguishability measure is very high over the whole space, except for the data points that fall right between the two mean

predictions $\mu_1$ and $\mu_2$. When the certainty in these predictions gets lower, the indistinguishability gap between the predictions is wider (Fig. 2, right).

Another example concerns the opposite case and is shown Fig. 3 (left): the models are hardly distinct, except if data points fall very far from the predicted means (the flatter of the two models is recognized). Finally, we show Fig. 3 (right) the general case of varying means and standard deviations.

### *a priori* distinguishability

A priori distinguishability is the analysis of models and their prediction, without reference to any actual experimental data point. In this paper, we have chosen to separate the data space in two components, $x$ and $y$, which have different practical interpretations. $x$ is the input data, that is to say, the part of the experimental point which is decided by the experimenter. On the other hand, $y$ is the output data, that is to say, the measure which is made in experimental condition $x$.

For instance, if studying free falling objects, $x$ might be weights, and $y$ the time that it takes for an object of weight $x$ to fall from the top of the tower of Pisa. When studying human memory, $x$ might be the time of presentation of a stimulus to a participant, and $y$ the number of features of that stimulus which are correctly recalled by the participant.

Having these two components in the data space opens two variants for *a priori* distinguishability. Firstly, it can be the distinguishability of models $M_1$ and $M_2$ for a given experimental condition $x$, without knowing $y$:

$$P(D \mid x\, M_1\, M_2\, \Theta_1\, \Theta_2),$$

which we refer to as the *a priori* distinguishability proper. It can also be the distinguishability of models $M_1$ and $M_2$ for all experimental conditions $x$ and possible outcomes $y$:

$$P(D \mid M_1\, M_2\, \Theta_1\, \Theta_2),$$

which we refer to as the *overall a priori* distinguishability.

Both can be obtained from a posteriori distinguishability by Bayesian inference from the hierarchical model of model comparison $P(D\, x\, y\, M_1\, M_2\, \Theta_1\, \Theta_2)$. Indeed, assuming uniform probability distributions over discrete $x$ and $y$ variables [3]:

$$P(D \mid x\, M_1\, M_2\, \Theta_1\, \Theta_2) \quad \propto \quad \sum_y P(D \mid x\, y\, M_1\, M_2\, \Theta_1\, \Theta_2),$$

$$P(D \mid M_1\, M_2\, \Theta_1\, \Theta_2) \quad \propto \quad \sum_{x,y} P(D \mid x\, y\, M_1\, M_2\, \Theta_1\, \Theta_2).$$

Fig. 4 shows the *a priori* distinguishability of two models that are based on Gaussian probability distributions, with means that are linear in $x$ and standard deviations that are constant, and equal between the two models:

$$P(y \mid x\, M = M_1) \quad = \quad \mathbf{G}_{\mu=\mathbf{a_1 x + b_1}, \sigma = \mathbf{k}}(\mathbf{y})$$

$$P(y \mid x\, M = M_2) \quad = \quad \mathbf{G}_{\mu=\mathbf{a_2 x + b_2}, \sigma = \mathbf{k}}(\mathbf{y})$$

[3]An interesting case would be to consider when $y$ is assumed to be distributed according to the average prediction given by all considered models: $P(y) = \sum_{x,M,\Theta} P(y \mid x\, M\, \Theta)$. We will not develop this further here.
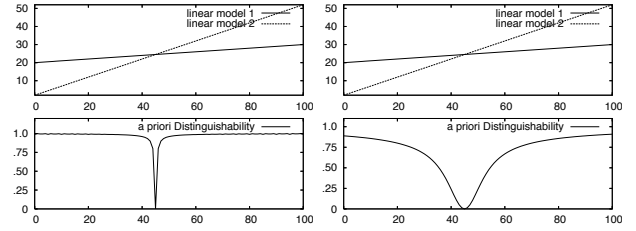


Figure 4: A priori distinguishability. Left: each model is linear with some normal noise of small standard deviation ($\sigma = 1.0$). As a result, models are easily distinguished in most of the space. Right: the noise is increased around the linear predictions ($\sigma = 5.0$): in the whole middle portion of the space, models are hardly distinguishable.

The left panel of Fig. 4 shows the case where the standard deviation $k$ is small for the two models, so that they are highly distinguishable for almost all input data $x$, except where the means get close, because the linear functions $a_1 x + b_1$ and $a_2 x + b_2$ cross. The right panel shows a similar case, where the standard deviations $\sigma = k$ are larger, so that the region where models are less distinguishable is larger.

The computation of the overall *a priori* distinguishability is not detailed here, but it is trivial that it yields a higher distinguishability for the two models on the left panel than for the two models of the right panel of Fig. 4.

## Full scale example: human arm control and planning strategies

Having illustrated the distinguishability model on a few mono-dimensional examples in previous sections, we now turn to a more complex scenario. We study here the planning and execution of movements for a two degree-of-freedom arm.

### Human arm geometric model and notation

We consider a simple model of the right human arm, using two segments of same unitary length and two joints, $\alpha_1$ the shoulder angle, and $\alpha_2$ the elbow angle. This arm is constrained to move in the horizontal plane, and its endpoint (wrist) position is described by its $x, y$ coordinates in this plane.

We only consider a limited range for possible arm configurations, that include biologically relevant positions: $\alpha_1$, the shoulder angle, ranges from $-\pi/6$ (arm extended behind the subject) to $5\pi/6$ (arm crossing, in front of the chest). The elbow goes from $\alpha_2 = 0$ when the arm is outstretched, to a maximum value which is function of the shoulder position: when the arm is away from the chest, we assume the elbow can bend totally ($\alpha_2 = \pi$), while when the arm is close to the chest, this restricts the elbow angle to decrease linearly with $\alpha_1$, so that when $\alpha_1$ is maximum, $\alpha_2$ only goes up to $\pi/2$.

The shoulder position is set at the origin $(x, y) = (0, 0)$. The set of possible angular joint configurations defines a
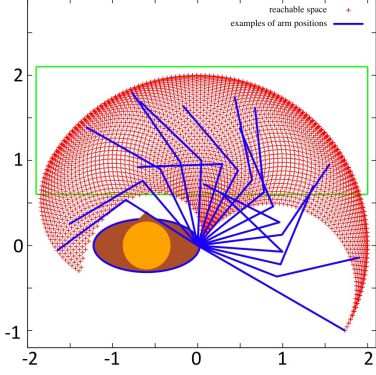
Figure 5: Overhead view of the horizontal plane, the reachable workspace (red or grey crosses), and some examples of possible arm configurations (blue or solid dark segments). The green square (light grey) delimits the integration space for computing the a priori distinguishability (see main text).

workspace of possible reachable positions for the endpoint, which is shown Figure 5. Each of these endpoint positions can be described either in the joint space by a pair of angular coordinates $\alpha_1, \alpha_2$, or in a Cartesian reference frame by the pair of $x, y$ endpoint coordinates in the workspace.

## Models of trajectory formation: interpolation in the joint space or in the workspace?

Movements in this two dimensional space are defined between a start position $S$ and an end position $E$. Trajectories between these points are assumed to take a unitary interval of time; in other words, each trajectory is indexed by a time variable $\tau$ that goes between 0 and 1, with $\alpha_1(0), \alpha_2(0)$ (or $x(0), y(0)$) being the start position $S$ and $\alpha_1(1), \alpha_2(1)$ (or $x(1), y(1)$) being the end position $E$.

There are two main hypotheses concerning the planning of movements in this context: movements might be planned in the articulatory or joint space (intrinsic planning), or they might be planned in the Cartesian workspace (extrinsic planning) (Palluel-Germain, Boy, Orliaguet, & Coello, 2006). We further assume, for these two alternatives, that the planning process is a simple linear interpolation (Hollerbach & Atkeson, 1987)

### Bayesian models $M_{int}$ and $M_{ext}$

Here, we define the two probabilistic models we consider.

The first model, $M_{int}$ assumes that movements are planned in the intrinsic reference frame. In other words, given start joint angular values $S = (\alpha_1(0), \alpha_2(0))$ and end joint angular values $E = (\alpha_1(1), \alpha_2(1))$, the trajectory to be followed is chosen so that, for all time index $\tau \in [0, 1]$, the joint values $\alpha_1(\tau), \alpha_2(\tau)$ are interpolated linearly between the start and end positions.

The start and end positions of movements constitute the $x$ "input" experimental condition of our data space. The chosen and planned trajectory is the output of this experimental point,

what the model is predicting; in order to simplify the computational analysis, we choose to summarize the whole planned trajectory by a single point along this trajectory, the one at time $\tau = 1/2$. Furthermore, we assume this point is observed in the Cartesian space $x, y$. In other words, the "output" data point, $y$, is the endpoint position $x_{int}(1, 2), y_{int}(1/2)$ reached at time $\tau = 1/2$ along the trajectory planned in intrinsic coordinates. Around this predicted position, we will assume some noise, normally distributed, using a two-dimensional gaussian probability distribution with mean $\mu_{int}$ and diagonal covariance matrix $S$:

$$\mu_{int} = \left[ \begin{array}{c} x(1/2) \\ y(1/2) \end{array} \right], \quad S = \left[ \begin{array}{cc} \sigma & 0 \\ 0 & \sigma \end{array} \right].$$

Finally, $M_{int}$ has no internal parameter $\Theta_{int}$, which simplifies the notation.

We can now make $M_{int}$ formal in the Bayesian programming notation:

$$
\begin{aligned}
&P(y \mid x\ M = M_{int}) \\
&\quad = \quad P(x\ y \mid \alpha_1(0)\ \alpha_2(0)\ \alpha_1(1)\ \alpha_2(1)\ M = M_{int}) \\
&\quad = \quad \mathbf{G}_{\mu,S}(x, y)
\end{aligned}
$$

The second model, $M_{ext}$, on the other hand, assumes that movements are planned in the extrinsic reference frame, that is to say, directly the Cartesian workspace. In other words, given start joint angular values $S = (\alpha_1(0), \alpha_2(0))$ and end joint angular values $E = (\alpha_1(1), \alpha_2(1))$, these are first converted into Cartesian start and end positions $x(0), y(0)$, $x(1), y(1)$. Then the straight segment, in the workspace, that connects these two points is the predicted trajectory. Trivially, the predicted middle point at time $\tau = 1/2$ is the geometric middle of the segment (assuming a symmetric velocity profile).

As previously, we assume some normally distributed noise around the middle of the segment $x_{ext}(1/2), y_{ext}(1/2)$:

$$
\begin{aligned}
&P(y \mid x\ M = M_{ext}) \\
&\quad = \quad P(x\ y \mid \alpha_1(0)\ \alpha_2(0)\ \alpha_1(1)\ \alpha_2(1)\ M = M_{ext}) \\
&\quad = \quad \mathbf{G}_{\mu_{ext},S}(x, y)
\end{aligned}
$$

We show Fig. 6 some examples of trajectories predicted by the intrinsic planning model $M_{int}$ and the extrinsic planning model $M_{ext}$, and the predicted points for the middles of these trajectories, at $\tau = 1/2$. A special case can be seen where the trajectories are superposed: this is when the line that passes by the start point $S$ and end point $E$ also passes through the shoulder position $(0, 0)$. As previously demonstrated, in this case of radial movements, the predicted trajectories are straight segments both in the intrinsic and extrinsic models (Hollerbach & Atkeson, 1987).

## Distinguishability of intrinsic and extrinsic interpolation models

Having defined the two intrinsic and extrinsic models in the Bayesian framework, by the terms $P(y \mid x\ M = M_{int})$ and
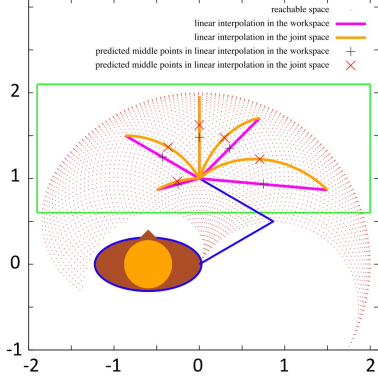
Figure 6: Some trajectories from the same starting position $S$: $\alpha_1(0) = \pi/6, \alpha_2(0) = 4\pi/6$, predicted by the intrinsic planning model $M_{int}$ (curved trajectories, in orange or light grey) and the extrinsic planning model $M_{ext}$ (straight segments, in purple or dark grey).

$P(y \mid x\ M = M_{ext})$, we can then encapsulate them in the Bayesian metamodel of distinguishability. This allows to compute, for each possible movement to be performed in the workspace, the *a priori* distinguishability between $M_{int}$ and $M_{ext}$.

More precisely, we restrict the considered movements to those that can be performed by both strategies. Indeed, because the reachable space is not convex (see Fig. 5 or Fig. 6) some movements do have solutions in the intrinsic model, but not in the extrinsic model. In other words, for some pairs of start and end positions, the segment between them lies outside of the reachable space. For instance, this is the case for trajectories with the arm fully outstretched at the starting position. For this reason, we restrict our analysis for a convex subregion of the reachable space (the green rectangle of Fig. 5), and only compute the distinguishability of models for movements where both the start and end positions are inside it.

For a given movement, defined by a start position $S = (\alpha_1(0), \alpha_2(0))$ and an end position $E = (\alpha_1(1), \alpha_2(1))$, we compute the *a priori* distinguishability of models $M_{int}$ and $M_{ext}$, by integrating over all possible data points. Here again, we only consider possible data points that fall inside the green rectangle of Fig. 5.

Therefore, we obtain, for all possible movements, the probability values $P(D = 1 \mid \alpha_1(0)\ \alpha_2(0)\ \alpha_1(1)\ \alpha_2(1)\ M_1 = M_{int}\ M_2 = M_{ext})$.

**Result analysis** However, since all possible movements define a four dimensional space, this distinguishability measure cannot easily be visualized and interpreted as is. Some selections and projections to lower dimensional spaces is required, for the distinguishability measure to be plotted. We will firstly present results for a given start position (for all possible end positions), and secondly, aggregated results for all possible pairs of start and end positions.

We further define three projections, to analyse the results.
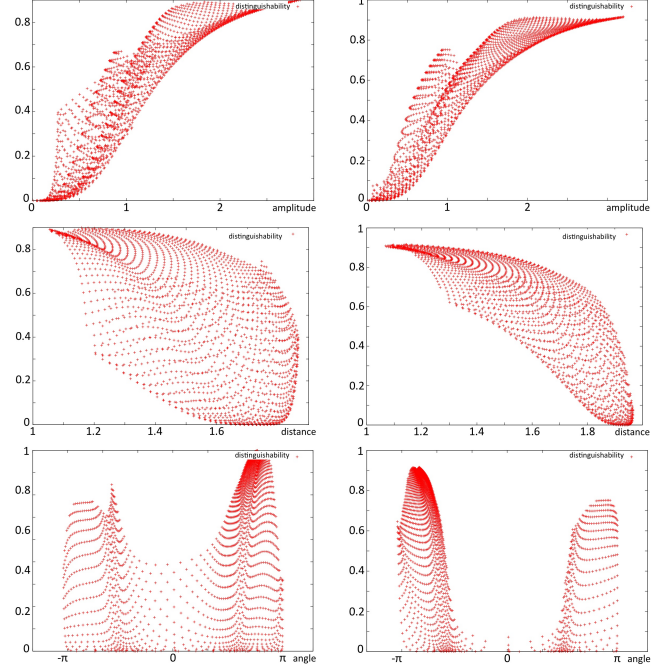


Figure 7: Top row: distinguishability of models plotted against the amplitude of a movement. Middle row: distinguishability of models plotted against the distance of a movement. Bottom row: distinguishability of models plotted against the angle difference with respect to radial lines. Left column: distinguishability of models for all possible movements starting from $S = (\pi/6, \pi/3)$. Right column: distinguishability of models for all possible movements starting from $S = (5\pi/8, \pi/6)$.

We will group movements according to their amplitude, their distance to the shoulder, and their angle difference with respect to radial lines.

The amplitude of a given movement from start position $S$ to end position $E$ is simply defined as the Cartesian distance between $S$ and $E$ in the workspace.

The distance of a given movement from start position $S$ to end position $E$ we define as the distance to origin of the point at $\tau = 1/2$ predicted by $M_{ext}$. In other words, we consider the distance between the shoulder position and the middle of the segment between $S$ and $E$ in the workspace: some movements are performed very near the body, some movements are performed near the outside limits of the workspace.

Finally, the angle difference with respect to radial lines, for a given movement from start position $S$ to end position $E$, we define as the angle difference between the segment $SE$ and the segment from shoulder position $(0,0)$ to $S$. This measure allows to see whether a given movement is purely radial (going straight away from or to the shoulder), or if it is a circular movement (tangent to some circle centered on the shoulder).

We show Fig. 7 the distinguishability analysis for three different starting positions. Fig. 8 shows the aggregate results for all possible starting positions.
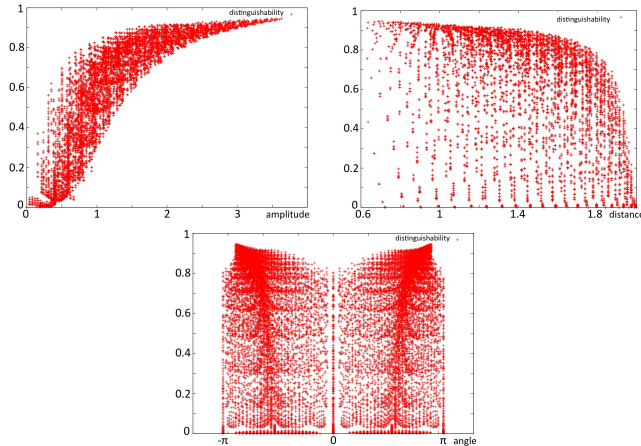
Figure 8: Distinguishability of $M_{int}$ and $M_{ext}$ for all possible movements. Top left plot: distinguishability plotted against the amplitude of movements. Top right plot: distinguishability plotted against the distance of movements. Bottom plot: distinguishability plotted against the angle difference with respect to radial lines.

**Result interpretation**  From these results, some conclusions can be drawn.

The most prominent feature is that the models $M_{int}$ and $M_{ext}$ appear to be most distinguishable when movements are large. Indeed, the distinguishability of models is high for movements of large amplitude, and gets to 0 when the movements are very small. This is confirmed easily by intuition: for large movements, the geometry of the arm has the most impact on the curve predicted by $M_{int}$. In other words, we see here the effect of the direct kinematic transform.

A second feature is that, for all possible movements, the distinguishability of models does not seem to be dependent of the distance of the performed movement. However, an exception is to be noted: when movements are performed near the outer boundary of the reachable space, the models become hardly distinguishable: their distinguishability dips to 0. This is a confirmation of a fact that was already demonstrated mathematically (Hollerbach & Atkeson, 1987). This was a very important finding, as it allowed to cast doubt on the discrimination power of a previous experiment, where participants had to perform movements bringing them to that outer boundary (Soechting & Lacquaniti, 1981).

A final feature we wish to analyze concerns the angle of movements with respect to radial lines. Contrary to the previous case, this finding contradicts, or rather refines, previous mathematical developments. Indeed, it was shown previously that purely radial movements render the intrinsic and extrinsic planning models not distinguishable (Hollerbach & Atkeson, 1987). Indeed, in this case, both models predict that the trajectories performed are straight (radial) segments. We also confirmed this in one of the example trajectories shown Fig. 6. However, this indistinguishability is purely spatial: when considering the time profile of trajectories, they become distinguishable. This is shown by the bottom plot of Fig. 8: while it is true that radial movements entail, overall, a slightly lower distinguishability of models, there are radial movements where $M_{int}$ and $M_{ext}$ are still distinguishable. This can also be demonstrated by isolating these trajectories, and analyzing them. And indeed, even for radial movements, the positions predicted at time $\tau = 1/2$ are different for the two models. This was also shown on the example radial trajectory of Fig. 6.

## Conclusion

In this paper, we developed an original Bayesian metamodel that integrates the notion of distinguishability of models. It allows to manipulate this concept using Bayesian inference, to compute a posteriori distinguishability of given models, but also their a priori and overall a priori distinguishability. We illustrated our model on an example about the planning of arm movements in humans, and showed how it could be used to analyse the space of all possible experimental points. For instance, it was shown that radial movements are indistinguishable spatially, are distinguishable in the temporal domain, and finally, that movements of large amplitude could be used to better discriminate between the alternative models of intrinsic and extrinsic planning.

Further theoretical developments include using the distinguishability metamodel to draw experimental conditions, given that we look for discriminating power, using Bayesian inference to compute a term of the form $P(x \mid M_1\ \theta_1\ M_2\ \theta_2\ D = 1)$.

## References

Berthier, F., Diard, J.-P., Pronzato, L., & Walter, E. (1996). Identifiability and distinguishability concepts in electrochemistry. *Automatica*, *32*(7), 973–984.

Hélie, S. (2005). An introduction to model selection: Tools and algorithms. *Tutorials in Quantitative Methods for Psychology*, *1*(1), 1–10.

Hollerbach, J., & Atkeson, C. G. (1987). Deducing planning variables from experimental arm trajectories: Pitfalls and possibilities. *Biological Cybernetics*, *56*, 279–292.

Myung, I. J., & Pitt, M. A. (2004). Model comparison methods. *Methods in Enzymology*, *383*, 351–366.

Navarro, D. J., Pitt, M. A., & Myung, I. J. (2004). Assessing the distinguishability of models and the informativeness of data. *Cognitive Psychology*, *49*, 47-84.

Palluel-Germain, R., Boy, F., Orliaguet, J.-P., & Coello, Y. (2006). Influence of visual constraints in the trajectory formation of grasping movements. *Neuroscience Letters*(401), 97–102.

Soechting, J., & Lacquaniti, F. (1981). Invariant characteristics of a pointing movement in man. *Journal of Neuroscience*, *1*, 710–720.